Wave-Structure-Soil Interaction (WSSI) Toolbox

Manual

Developed for
FOAM-extend-3.1,
FOAM-extend-4.0

Author:
Yuzhu (Pearl) LI
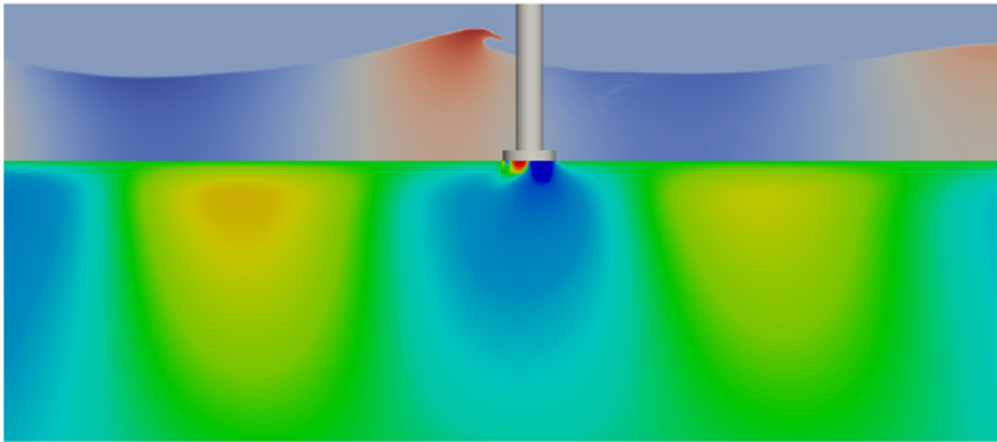
April 19, 2021

Referencing

The users are requested to support the work put into the `wssi` toolbox by providing proper referencing to the academic works. Any use of `wssi` toolbox: Please make reference to the original work (Li et al. 2020) as follows:

- Li, Y., Ong, M. C., & Tang, T. (2020). A numerical toolbox for wave-induced seabed response analysis around marine structures in the OpenFOAM® framework. Ocean Engineering, 195, 106678.

In Bibtex format:

```
@article{li2020numerical,
  title={A numerical toolbox for wave-induced seabed response analysis around
  marine structures in the {O}pen{FOAM}{\textregistered} framework},
  author={Li, Yuzhu and Ong, Muk Chen and Tang, Tian},
  journal={Ocean Engineering},
  volume={195},
  pages={106678},
  year={2020},
  publisher={Elsevier}
}
```

Contents

Chapter 1

Download and installation

1.1 Work environment

To install the wssi solvers, you will need to have `FOAM-extend-3.1` or the `FOAM-extend-4.0` installed in your Linux system. Check the following links for the instructions to install the foam-extend projects:

https://openfoamwiki.net/index.php/Installation/Linux/foam-extend-3.1
https://openfoamwiki.net/index.php/Installation/Linux/foam-extend-4.0

1.2 Download solvers

In the WSSI analysis, the structure and soil solvers will read wave pressure data from a free-surface solver. There is no restriction on selecting the free-surface modeling tools. In the OpenFOAM CFD library, various solvers can be adopted, such as `interFoam` solver in OpenFoam, toolboxes of `waves2Foam` (Jacobsen et al., 2012) and `iHFoam` (Higuera et al., 2013). In the tutorial works, the `waves2Foam` is adopted for modeling the wave generation and absorption. For `waves2Foam` installation, users can refer to the link: https://openfoamwiki.net/index.php/Contrib/waves2Foam.

To download the `wssi` structure and soil solvers and tutorials:

```
git clone https://github.com/LiYZPearl/wssi
```

1.3 Installation

```
cd wssi/wssi-fe-3.1/
chmod u+x Allwmake
./Allwmake
```

Chapter 2

Introduction to the toolbox

2.1 Theoretical background

2.1.1 Free Surface Wave Model

In the wave-structure-seabed analysis, the wave domain is governed by the incompressible Navier-Stokes equations including the continuity equation and the momentum equations.

$$\nabla \cdot \mathbf{u} = 0 \tag{2.1}$$

$$\frac{\partial \mathbf{u}}{\partial t} + (\mathbf{u} \cdot \nabla)\mathbf{u} = -\frac{1}{\rho_f}\nabla p_d + \mathbf{g} + \frac{1}{\rho_f}\nabla \cdot \boldsymbol{\tau} \tag{2.2}$$

where $\mathbf{u}$ denotes the velocity vector with three components in the x,y,and z directions respectively; $\mathbf{g}$ denotes the gravitational acceleration; ρ_f is the fluid density which can represent the air ρ_a or the water ρ_w. p_d is the dynamic wave pressure which is defined as $p_d = p_t - \rho_f \mathbf{g} \cdot \mathbf{x}$, where p_t is the total pressure and the $\mathbf{x} = (x, y, z)$ is the Cartesian coordinate vector. $\boldsymbol{\tau}$ is the viscous stress tensor with Einstein notation of τ_{ij}. For Newtonian fluid,

$$\tau_{ij} = 2\mu\sigma_{ij} \tag{2.3}$$

where μ is the dynamic molecular viscosity with μ_{air} for the air and μ_{water} for the water. σ_{ij} is defined by

$$\sigma_{ij} = \frac{1}{2}\left(\frac{\partial u_i}{\partial x_j} + \frac{\partial u_j}{\partial x_i}\right) \tag{2.4}$$

where $i, j \in [1,2,3]$. u_i and u_j denote the velocity components in x, y and z direction respectively.

The equations are solved for the two immiscible fluids simultaneously, where the fluids are tracked using a scalar field α. α is 0 for air and 1 for water, and any intermediate value is a mixture of the two fluids. The distribution of α is modelled by an advection equation

$$\frac{\partial \alpha}{\partial t} + \nabla \cdot \alpha\mathbf{u} + \nabla \cdot [\alpha(1-\alpha)\mathbf{u}_r] = 0 \tag{2.5}$$

The last term on the left-hand side is a compression term, which limits the smearing of the interface, and $\mathbf{u}_r$ is a relative velocity (Berberović et al., 2009).

Using α, one can express the spatial variation in any fluid property, through the weighting

$$\Phi = \alpha\Phi_{water} + (1-\alpha)\Phi_{air} \tag{2.6}$$

Φ is a fluid property, such as ρ_f and μ.

2.1.2 Linear Elastic Structure Model

The structure domain is modelled as a linear elastic media and is governed by a linear momentum balance equation and isotropic linear elastic strain-displacement relations (Li et al., 2018).

$$\nabla \cdot \boldsymbol{\sigma} = \nabla \cdot [2\mu\boldsymbol{\epsilon} + \lambda \mathrm{tr}(\boldsymbol{\epsilon})\mathbf{I}] = 0 \tag{2.7}$$

$$\boldsymbol{\epsilon} = 1/2(\nabla\mathbf{U} + \nabla\mathbf{U}^T) \tag{2.8}$$

where $\boldsymbol{\sigma}$ is the stress tensor; $\boldsymbol{\epsilon}$ is the small strain tensor; $\mathbf{U}$ is the structural displacement vector consisting of three coupled components. μ and λ are the Lamé's coefficients of elastic material properties, relating to more commonly used Young's modulus E and Poisson's ratio ν.

In the FVM analysis, the coupling of the three displacement components U_x, U_y, U_z are handled by using the segregated strategy Demirdžić and Martinović (1993); Demirdžić and Muzaferija (1994). Substitute Eqn. 2.8 into Eqn. 2.7 and the combined equation can be split into an implicit part and an explicit part, shown in Eqn. 2.9.

$$\nabla \cdot [(2\mu + \lambda)\nabla\mathbf{U}] = -\nabla \cdot [\mu(\nabla\mathbf{U})^T + \lambda\mathbf{I}\mathrm{tr}(\nabla\mathbf{U} - (\mu + \lambda)\nabla\mathbf{U}] \tag{2.9}$$

The left hand side of the equation is the implicit part and the right hand side of the equation is the explicit part. Equation 2.9 is solved iteratively until the explicit terms essentially become implicit based on a fixed-point interaction algorithm (Jasak and Weller, 2000).

2.1.3 Anisotropic Poro-Elastic Soil Model

In the present work, the soil behavior is modelled by the classical Biot's consolidation equations (Biot, 1941) with the interaction between the solid skeleton and the pore fluids, considering the anisotropic soil characteristics. The seabed is nearly saturated and the soil skeleton generally obeys Hooke's law with elastic properties.

Constitutive relations

In the present work, the tension stress is defined as positive while the compression stress is defined as negative, in compliance with the tradition in computational continuum mechanics. The total stress for the saturated porous medium is defined by

$$\boldsymbol{\sigma} = \boldsymbol{\sigma}' - p\mathbf{I} \tag{2.10}$$

where $\boldsymbol{\sigma}'$ is the effective stress tensor of the soil skeleton, $\boldsymbol{\sigma}$ is the total stress tensor of soil mixture, p is the pore fluid pressure, and $\mathbf{I}$ is the identity tensor.

Effective stress-strain relation by the generalized Hooke's law is expressed as

$$\boldsymbol{\sigma}' = C : \boldsymbol{\varepsilon} \tag{2.11}$$

The strain-displacement relation is expressed as

$$\boldsymbol{\varepsilon} = \frac{1}{2}(\nabla\mathbf{U} + (\nabla\mathbf{U})^T) \tag{2.12}$$

where $\boldsymbol{\varepsilon}$ is the strain tensor, $\mathbf{U}$ is the soil skeleton displacement vector.

For anisotropic soil materials, the orthotropic elastic stress-strain relation can be expressed in a 6×6 matrix notation:

$$\boldsymbol{\sigma}' = \begin{pmatrix} \sigma'_{xx} \\ \sigma'_{yy} \\ \sigma'_{zz} \\ \sigma_{xy} \\ \sigma_{yz} \\ \sigma_{xz} \end{pmatrix} = \begin{bmatrix} A_{11} & A_{12} & A_{31} & 0 & 0 & 0 \\ A_{12} & A_{22} & A_{23} & 0 & 0 & 0 \\ A_{31} & A_{23} & A_{33} & 0 & 0 & 0 \\ 0 & 0 & 0 & A_{44} & 0 & 0 \\ 0 & 0 & 0 & 0 & A_{55} & 0 \\ 0 & 0 & 0 & 0 & 0 & A_{66} \end{bmatrix} \begin{pmatrix} \varepsilon_{xx} \\ \varepsilon_{yy} \\ \varepsilon_{zz} \\ \varepsilon_{xy} \\ \varepsilon_{yz} \\ \varepsilon_{xz} \end{pmatrix} = \mathbf{C} : \boldsymbol{\varepsilon} \tag{2.13}$$

where $\boldsymbol{\sigma}'$ is the effective stress tensor. According to the work of Demirdžić et al. (2000), the 9 independent coefficients A_{ij} are calculated from Young's modulus E_i and Poisson's ratio ν_{ij} and shear modulus G_{ij} as follows:

$$
\begin{aligned}
A_{11} &= \frac{1 - \nu_{yz}\nu_{zy}}{JE_yE_z}, & A_{22} &= \frac{1 - \nu_{xz}\nu_{zx}}{JE_xE_z}, & A_{33} &= \frac{1 - \nu_{yx}\nu_{xy}}{JE_yE_x}, \\
A_{12} &= \frac{\nu_{xy} + \nu_{zy}\nu_{xz}}{JE_xE_z}, & A_{23} &= \frac{\nu_{yz} + \nu_{yx}\nu_{xz}}{JE_xE_y}, & A_{31} &= \frac{\nu_{zx} + \nu_{yx}\nu_{zy}}{JE_yE_z}, \\
A_{44} &= 2G_{xy}, & A_{55} &= 2G_{yz}, & A_{66} &= 2G_{zx}
\end{aligned}
\tag{2.14}
$$

where

$$
J = \frac{1 - \nu_{xy}\nu_{yx} - \nu_{yz}\nu_{zy} - \nu_{xz}\nu_{zx} - 2\nu_{yx}\nu_{zy}\nu_{xz}}{E_xE_yE_z}
\tag{2.15}
$$

Quasi-static model for consolidation analysis

The Biot's model contains two governing partial differential equations: One vector equation for the momentum equilibrium. One scalar equation for the mass conservation.

In the consolidation analysis, a static gravitational force is imposed on the seabed; therefore, the Biot's model in the quasi-static form is applied because the frequency of the process is very low. The soil domain in the consolidation analysis is governed by a quasi-static momentum balance equation for the soil mixture and a mass balance equation for the pore fluid based on Darcy's law. The quasi-static momentum balance equation is presented in Eqn. 2.16:

$$
\nabla \cdot [\mathbf{C} : \frac{1}{2}(\nabla\mathbf{U} + (\nabla\mathbf{U})^T)] - \nabla p + \rho\mathbf{g} = 0
\tag{2.16}
$$

where $\mathbf{U}$ is the soil (skeleton) displacement, p is the pore fluid pressure, ρ is the density of the soil mixture, $\mathbf{g}$ is the gravitational acceleration vector with components of $(0, 0, g)$, and $\mathbf{C}$ is the fourth-order elastic stiffness tensor. The density of the soil mixture, or submerged density of the soil is calculated by

$$
\rho = n\rho_f + (1 - n)\rho_s
\tag{2.17}
$$

where n is the porosity, ρ_s is the soil density and ρ_f is the water density.

The mass balance equation of the pore fluid based on Darcy's law is shown in Eqn. 2.18:

$$
\frac{n}{K'}\frac{\partial p}{\partial t} - \frac{1}{\gamma_w}\nabla \cdot (\mathbf{k} \cdot \nabla p) + \frac{\partial}{\partial t}(\nabla \cdot \mathbf{U}) + \frac{\mathbf{k}}{g} \cdot (\nabla \cdot \mathbf{g}) = 0
\tag{2.18}
$$

where n denotes the soil porosity, γ_w denotes the specific weight of water in soil, and $\mathbf{k}$ denotes the diagonal permeability tensor with values of k_x, k_y and k_z. The bulk modulus of the compressible pore flow K' is approximately computed by using the formulation of Vafai and Tien (1981):

$$
\frac{1}{K'} = \frac{1}{K_w} + \frac{1 - S_r}{p_a}
\tag{2.19}
$$

where S_r denotes the degree of soil saturation, K_w denotes the bulk modulus of pure water ($\approx$ 2GPa), and $p_a = \rho_f g h_w$ denotes the absolute pore water pressure at the seabed.

u-p approximation model for wave-induced seabed response

The partial dynamic $u - p$ formulation is more accurate compared to the quasi-static form for the oscillating problems and is more efficient compared to the fully-dynamic form for most of the engineering problems. Therefore, it is adopted for the wave-induced seabed response modeling in the present work. Satisfactory accuracy has been reported by the previous work such as Ye et al. (2013).

The wave-induced soil response analysis starts from the status that the gravity structure has been installed in place and the consolidation process has been completed. At this stage, the seabed soil

has adjusted itself in equilibrium with the massive weight of the gravity structure. The governing equations for the $u-p$ approximation model to analyze the wave effect on the soil is given as follows:

$$\nabla \cdot [\mathbf{C} : \frac{1}{2}(\nabla \mathbf{U} + (\nabla \mathbf{U})^T)] - \nabla p - \rho \frac{\partial^2 \mathbf{U}}{\partial t^2} = 0 \qquad (2.20)$$

$$\frac{n}{K'}\frac{\partial p}{\partial t} - \frac{1}{\gamma_w}\nabla \cdot (\mathbf{k} \cdot \nabla p) + \frac{1}{g}\nabla \cdot (\mathbf{k} \cdot \frac{\partial^2 \mathbf{U}}{\partial t^2}) + \frac{\partial}{\partial t}(\nabla \cdot \mathbf{U}) = 0 \qquad (2.21)$$

It is noted that the gravitational term $\rho\mathbf{g}$ is not incorporated in Eqn. 2.20 for the force balance. It is because that the partial dynamic $u-p$ approximation form is applied for the pure wave-induced soil response analysis, which starts from an equivalent status between the structure and the soil. Therefore, in the Eqn. 2.20, the external force is only the dynamic wave pressure, incorporated in the term p.

2.1.4 Liquefaction Criteria

As mentioned in Li et al. (2020b), there are various liquefaction criteria in the open literature based on the effective stress (Tsai, 1995; Okusa, 1985) or the excess pore pressure (Zen and Yamazaki, 1990b; Jeng, 1997). Ye (2012) compared different liquefaction criteria for the seabed without marine structure built on it. Ye (2012) concluded that among those liquefaction criteria based on the effective stress, the criteria of Okusa (1985) provides most appropriate engineering solution, while among those liquefaction criteria based on the excess pore pressure, the criteria of Zen and Yamazaki (1990b) provide the best engineering solution.

However, the criteria above are only applicable to the cases without a structure. In the case of liquefaction around a gravity structure, the initial effective stress from the consolidation stage should be taken into consideration. In the present soil solvers, modified liquefaction criteria considering the presence of the structure are incorporated in the liquefaction assessment module, including:

1. Criterion A. The modified form from Okusa (1985),

$$\sigma_z' \geq |\sigma_{z0}'| \qquad (2.22)$$

where σ_{z0}' is the initial vertical effective stress induced by the gravitational forces from the consolidation process.

2. Criterion B. The modified form from Zen and Yamazaki (1990b),

$$p - p_b \geq |\sigma_{z0}'| \qquad (2.23)$$

where p_b is the wave-induced pressure on the seabed surface.

The right hand sides of Eqn. 2.22 and Eqn. 2.23 express the downward gravitational forces including the soil weight and the external gravitational forces. The left hand sides of the liquefaction equations express the upward wave-induced hydraulic forces. It is worthwhile to mention that in the presence of the structure, especially when the structure is constructed on the loose seabed soil, nonlinear interaction between the seabed and the structure can occur. Therefore, the present liquefaction criteria can be no longer applicable.

2.1.5 Finite Volume Method Based Approach

In the Biot's model, the momentum and mass balance equations are strongly coupled. In the FVM analysis, the coupling of the three displacement components U_x, U_y, U_z and pressure p are handled by using a 'segregated strategy' (Demirdžić and Martinović, 1993; Demirdžić and Muzaferija, 1994). The equations are split into the 'implicit' and 'explicit' discretization parts, where the 'explicit' parts contain all the coupling effect from the other variables and shall be evaluated from the previous iteration or the initial condition.

The cross-component coupling in Eqn. 2.13 can be decomposed into implicit and explicit components:

$$\boldsymbol{\sigma}' = \mathbf{C} : \boldsymbol{\varepsilon} = \underbrace{\mathbf{K} \cdot \nabla \mathbf{U}}_{\text{implicit}} + \underbrace{\mathbf{C} : \boldsymbol{\varepsilon} - \mathbf{K} \cdot \nabla \mathbf{U}}_{\text{explicit}}. \tag{2.24}$$

where the $\mathbf{K}$ is a 3×3 diagonal stiffness tensor given by

$$\mathbf{K} = \begin{bmatrix} A_{11} & 0 & 0 \\ 0 & A_{22} & 0 \\ 0 & 0 & A_{33} \end{bmatrix} \tag{2.25}$$

In this way, Eqn. 2.16 and Eqn. 2.18 can be rearranged into the FVM implicit-explicit format:

$$\underbrace{\nabla \cdot (\mathbf{K} \nabla \mathbf{U})}_{\text{implicit}} = \underbrace{\nabla \cdot [\mathbf{C} : \frac{1}{2}(\nabla \mathbf{U} + \nabla \mathbf{U}^T)] + \nabla \cdot (\mathbf{K} \nabla \mathbf{U}) - \nabla p + \rho \mathbf{g}}_{\text{explicit}} \tag{2.26}$$

$$\underbrace{\frac{n}{K'} \frac{\partial p}{\partial t} - \frac{1}{\gamma_w} \nabla \cdot (\mathbf{k} \cdot \nabla p)}_{\text{implicit}} = \underbrace{-\frac{\partial}{\partial t}(\nabla \cdot \mathbf{U}) - \frac{\mathbf{k}}{g} \cdot (\nabla \cdot \mathbf{g})}_{\text{explicit}} \tag{2.27}$$

Similarly, the FVM implicit-explicit format for the $u - p$ approximation model to apply to the wave effect analysis is written as:

$$\underbrace{\nabla \cdot (\mathbf{K} \nabla \mathbf{U})}_{\text{implicit}} = \underbrace{\nabla \cdot [\mathbf{C} : \frac{1}{2}(\nabla \mathbf{U} + \nabla \mathbf{U}^T)] + \nabla \cdot (\mathbf{K} \nabla \mathbf{U}) - \nabla p - \rho \frac{\partial^2 \mathbf{U}}{\partial t^2}}_{\text{explicit}} \tag{2.28}$$

$$\underbrace{\frac{n}{K'} \frac{\partial p}{\partial t} - \frac{1}{\gamma_w} \nabla \cdot (\mathbf{k} \cdot \nabla p)}_{\text{implicit}} = \underbrace{-\frac{\partial}{\partial t}(\nabla \cdot \mathbf{U}) - \frac{1}{g} \nabla \cdot (\mathbf{k} \cdot \frac{\partial^2 \mathbf{U}}{\partial t^2})}_{\text{explicit}} \tag{2.29}$$
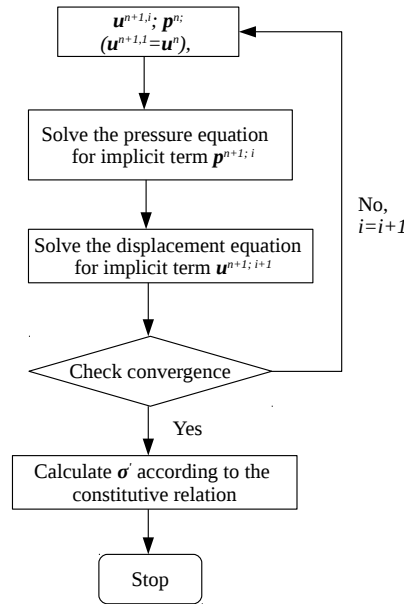

Figure 2.1: Iteration procedure for solving the Biot's model.

The iterative procedure for solving the Biot's models are shown in Fig. 2.1. Equations are solved iteratively until the solution changes less than a pre-defined tolerance. As pointed out in the work of Jasak and Weller (2000), the finite-volume(FV) discretization to the linear stress analysis problem uses small matrices for the three components of displacement, rather than using one large matrix that seen in the FEM. In this way, the usage of the computer memory can be significantly reduced.

2.2 The toolbox and its solvers

2.2.1 The toolbox

The present FVM-based toolbox can be applied to soil consolidation analysis, wave-structure-soil interaction (WSSI) analysis, and liquefaction assessment with and without structures. The current liquefaction assessment will be focused on the momentary (instantaneous) liquefaction using various criteria. The residual liquefaction assessment module will be released once it is validated.

An outline of the toolbox with included solvers is shown in Fig. 2.2.
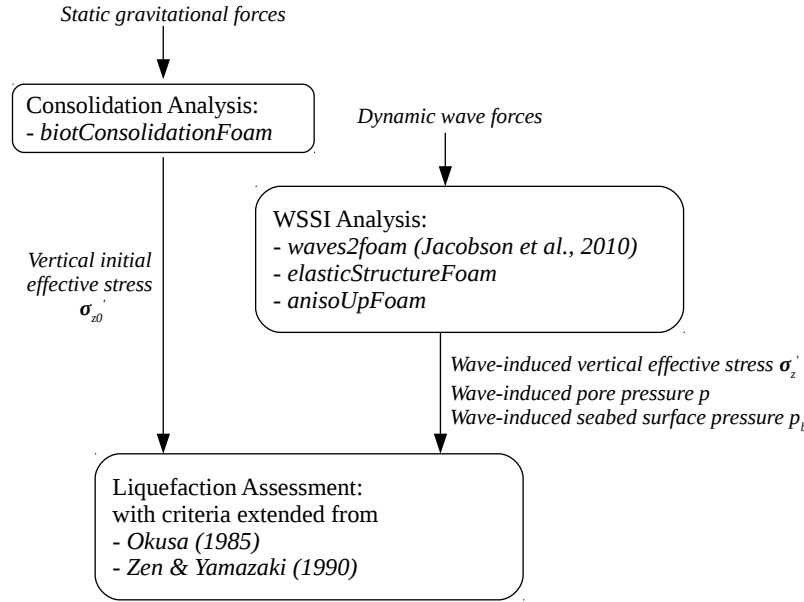

Figure 2.2: An outline of the WSSI toolbox.

- For the soil consolidation analysis, the solver named `biotConsolidationFoam` is developed. It reads the static gravitational force from the structure and computes the initial vertical effective stress in the soil. A detailed diagram is presented in Fig. 2.3.

- For the WSSI analysis, a diagram is presented in Fig. 2.4 using one-way coupling algorithm. In the WSSI analysis, the structure and soil solvers will read wave pressure data from a free-surface solver. There is no restriction on selecting the free-surface modeling tools. In the OpenFOAM CFD library, various solvers can be adopted, such as `interFoam` solver in OpenFoam, toolboxes `waves2Foam` (Jacobsen et al., 2012) or `iHFoam` (Higuera et al., 2013). In the tutorial works, the `waves2Foam` is adopted for modeling the wave generation and absorption.

- The structure solver `elasticStructureFoam` is developed in the work of Tang et al. (2014). It is an elastic structure solver which can read the wave pressure and compute the structural stresses.

- The soil solver named `anisoUpFoam` (renamed to `upFoam` in the updated package) is developed to consider the anisotropic soil property and the inertial force of the soil skeleton using the partial-dynamic (u-p) form of Biot's equation.

- For the liquefaction assessment, a function is written in the soil solver which reads data from the consolidation analysis and the WSSI analysis. Criteria extended from Okusa (1985) and Zen and Yamazaki (1990a) are implemented. Since the toolbox is based on the poro-elastic soil model, the momentary liquefaction is assessed. The liquefied area is marked with Flag 1 and non-liquefied area is marked with Flag 0 in the simulation.
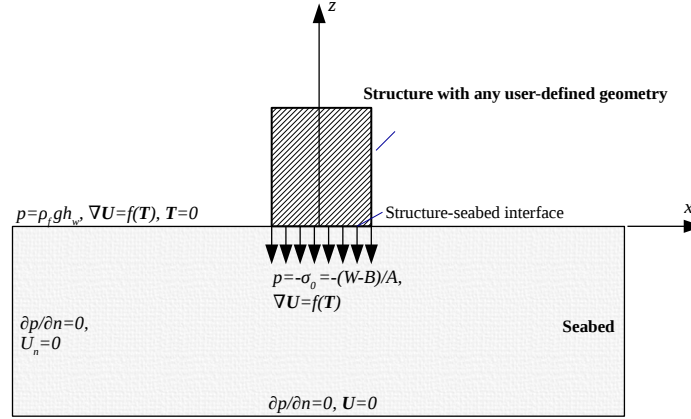

Figure 2.3: Boundary conditions of the consolidation analysis.

For solving the multiphysics WSSI problems, different physical domains can have different demands on the time step and grid size, based on the convergence and stability requisitions. For the WSSI problem, the time steps and the grid sizes needed for the linear-elastic soil and structural domains are relatively larger than what is needed for the nonlinear wave domain(Li, 2016). Therefore, it not efficient to calculate the multiple domains with the same grid size and to loop at the same time step. In the present model, time-dependent (time-varying) boundary conditions are applied for the data mapping at the interfaces. First, the values at the interfaces of the supplied domain are interpolated in space and time. Then, the interpolated values are mapped to the targeted domain interface with a reversed normal vector. In the present work, linear interpolation is applied. The boundary data are first interpolated in space for every face center and then interpolated linearly between the time instants.

2.2.2 Description of the available poro-elastic soil solvers

- `biotConsolidationFoam`

  This solver is based on the quasi-static Biot's model to solve the soil consolidation status under external static forces e.g. gravitational forces from structures. The input is the external stresses, and outputs are the initial effective soil stresses, soil displacements and pore pressure distributions during the consolidation process. The soil self-gravity is considered in the governing equations.

- `upFoam`

  This solver is based on the u-p approximation (partial-dynamic) soil model. It can be applied to examine the soil response under waves without the existence of structures. It reads the external wave forces (dynamic wave pressure) and computes the dynamic effective soil stresses,
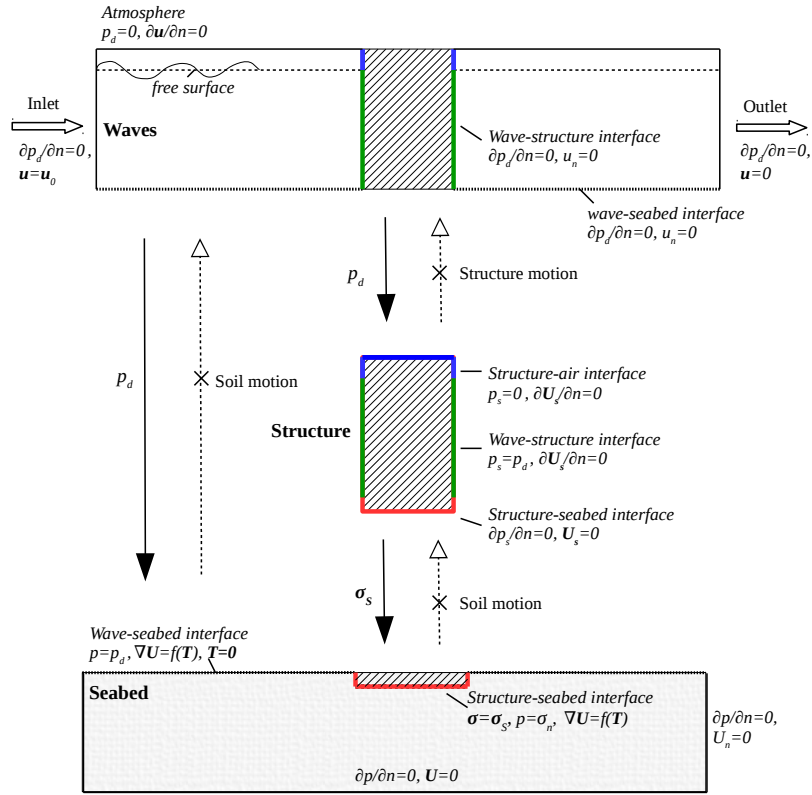
Figure 2.4: Boundary conditions of wave-structure-seabed interaction (WSSI) model and the one-way boundary coupling algorithm.

soil displacements and pore pressure distributions. It is noted that the gravitational term $\rho\mathbf{g}$ is not incorporated in the governing equations. This is because that this solver is for analyzing the pure wave-induced soil responses, which starts from an equilibrium status of the soil. Therefore, the external force is only the dynamic wave pressure, incorporated in the term p.

- `anisoBiotLiqueFoam`

  This solver is based on the quasi-static Biot's model to examine the soil responses in the presence of waves and structures. It is used for analyzing wave-structure-seabed interaction and liquefaction risk.

- `anisoUpLiqueFoam`

  This solver is based on the u-p approximation (partial-dynamic) Biot's model to examine the soil responses in the presence of waves and structures. It is used for analyzing wave-structure-seabed interaction and liquefaction risk.

2.2.3 One-way coupling

In the dynamic wave-structure-seabed interaction analysis, one-way coupling algorithm is considered, based on the assumption of small magnitudes of wave-induced structure vibration and soil deformations. In the one-way coupling WSSI, each domain is computed by sequence, instead of simultaneously.

- First the wave domain is calculated to get the dynamic wave pressure distribution on the structure and seabed. The wave pressure data are sampled and transformed to boundary data.

- Then the structure domain is solved using the boundary data of wave pressure as input. The seabed below it is assumed to be static. The structure stress at the structure-seabed interface is sampled and transformed to boundary data for the soil computation.

- Finally the soil domain is solved using the boundary data from wave domain (dynamic wave pressure at the wave-soil interface) and the structure domain (structural stress at the structure-seabed interface).

2.2.4 Boundary conditions

- `timeVaryingMappedFixedValue`

  This is a time-varying, non-uniform `OpenFOAM` boundary, which can read those sampled surface data (in the directory of /constant/boundaryData) such as dynamic wave pressure on the seabed and assign the corresponding values to the pore pressure field. When using this boundary, the `interpolationScheme` in sampleDict should use cellPoint.

- `externalPatchToPatchMapping`

  This is a time-varying, non-uniform boundary, equivalent to `timeVaryingMappedFixedValue`. However, this derived boundary uses the face mapping instead of the point mapping. This boundary is more robust for mapping curved faces, based on the tests. When using this boundary, the `interpolationScheme` in sampleDict should use cell instead of cellPoint (see the tutorials). This boundary is developed in foam-extend-3.1. When compiling the solvers in foam-extend-4.0, simply comment out the line below in /Make/files.

  `boundaries/externalPatchToPatchMapping/externalPatchToPatchMappingFvPatchFields.C`

- `timeVaryingMappedTotalTraction`

  This is a derived traction boundary which reads the time and spatial varying force data (from pressure p and/or stresses σ_S) and computes the traction load and compatible displacement gradient boundary. This boundary condition is derived from tractionDisplacement + timeVaryingMappedFixedValue in `OpenFOAM`.

- `fixedTraction`

  This is a derived traction boundary which reads the uniform force data (from pressure and/or stresses) and computes the traction load and compatible displacement gradient boundary.

For other boundary conditions used in the tutorials, please refer to OpenFOAM user guide.

Chapter 3

Tutorials

3.1 Consolidation

3.1.1 1D Terzaghi

In Terzaghi's classical consolidation test, a constant stress $-\sigma_0$ is applied on the surface $z = 0$ of a saturated sample of length L_s. Here, z is positive in the downward direction. The piston applying the load is permeable so that the top boundary is drained. The sample consolidates gradually as fluid flows out from the top drain. The setup of the test is shown in Fig. 3.1. The input parameters for the present numerical simulation is presented in Table 3.1.
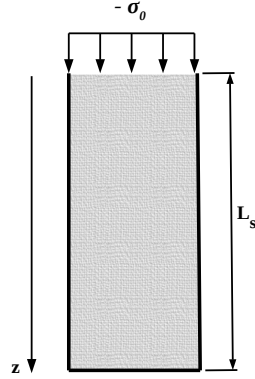

Figure 3.1: Test setup of Terzaghi's classical consolidation test.

Table 3.1: Parameter setting in the present numerical simulation for the 1D Terzaghi's consolidation test

Parameters	Values
L_s (m)	20
σ_0 (kPa)	10
Permeability k (m/s)	10^{-5}
Youngs modulus E (N/m^2)	10^8
Saturation degree S_r	0.995
Poissonsratio ν	0.25
Porosity n	0.3

The boundary conditions for reproducing the test is specified as follows:

14

At $z = 0$,

$$\sigma_z = -\sigma_0, \quad p = 0 \tag{3.1}$$

At $z = L_s$,

$$\frac{\partial p}{\partial z} = 0, \quad u_z = 0 \tag{3.2}$$

At four sides of the column, the boundary condition is defined as 'empty', i.e., the x and y directions are not solved, to achieve a one-dimensional problem. Detailed results and discussion can be seen in Li et al. (2020b).

Note that in the tutorial, the external static force at the top boundary where $z = 0$ is read from boundary data for `sigma_S` in the directory of constant/boundaryData/. The user can equivalently set 0/`sigma_S:boundaryField`:

```
top
{
    type      fixedValue;
    value     uniform (0 0 0 0 0 -10000);
}
```

3.1.2 Breakwater with berms

This tutorial case is described in the paper of Celli et al. (2019). As shown in Fig. 3.2, the berms deployed at the toe of the breakwater are built with rocks, loading the soil in a discontinuous way. The deployment of the breakwaters can significantly increase the effective stresses in the surrounding soil. Once built on the seabed, the self-weight of a breakwater with berms is initially transferred to the pore water in the seabed foundation, resulting in the generation of excess pore pressure. Then, the soil will experience the gradual dissipation of the excess pore pressure. Consequently, the breakwater load is gradually transferred from the pore water to the soil skeleton. At the end of the process, the seabed foundation reaches an equilibrium consolidation status. The final consolidation status is presented in Fig. 3.3. For more results and discussion, please refer to Celli et al. (2019).
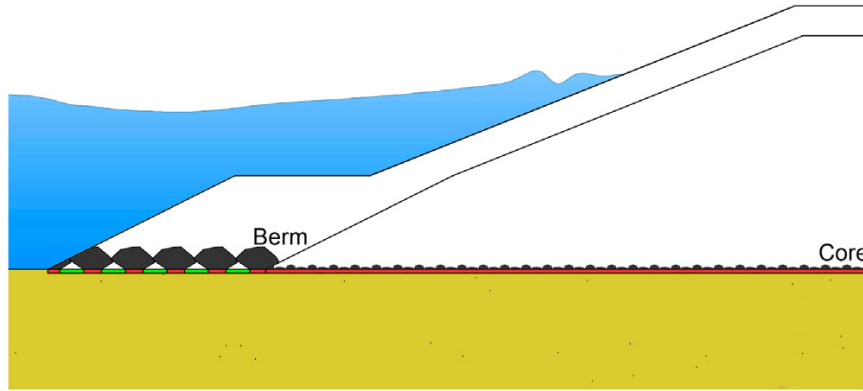

Figure 3.2: Sketch of breakwater with berms. Assumed load distribution under the porous structure: red zones refer to contact areas, where the load is transferred to the soil. Green zones refer to unloaded areas. Figure from Celli et al. (2019).
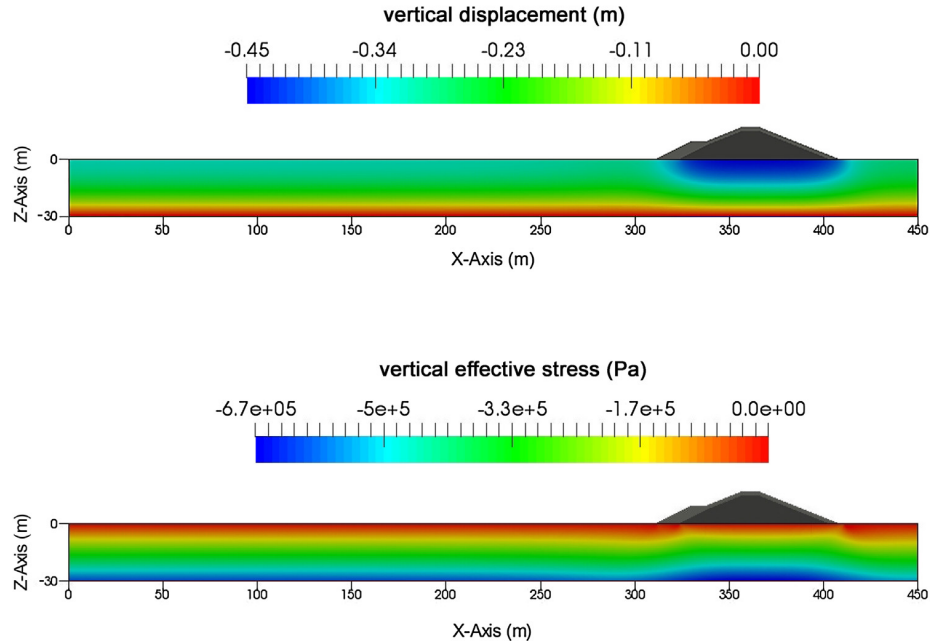
Figure 3.3: Consolidation process results of a breakwater with submerged berm. Figure from Celli et al. (2019).

3.2 2D wave-soil interaction

A two-dimensional (2D) wave-soil interaction case is provided in the tutorial. The steps to run this case are as follows:

1. Simulate waves (download `waves2foam`, compile in foam-extend-3.1 or use `interFoam` solver).

2. Sample the dynamic wave pressure on the seabed. Use the command

```
sample
```

3. Transform the format of surfaces data to boundary data. A shell script is provided in the tutorial as

```
./boundaryDataTransfer_seabed
```

Users can use any means to do the format transfer e.g. python or matlab.

4. Setup the soil case, copy the boundaryData folder to the soil/constant/. Use the soil solver:

```
upFoam
```

to calculate the stress, displacement and pressure distributions in the soil domain.

A snapshot of the simulation including wave and soil domains are presented in Fig. 3.4.
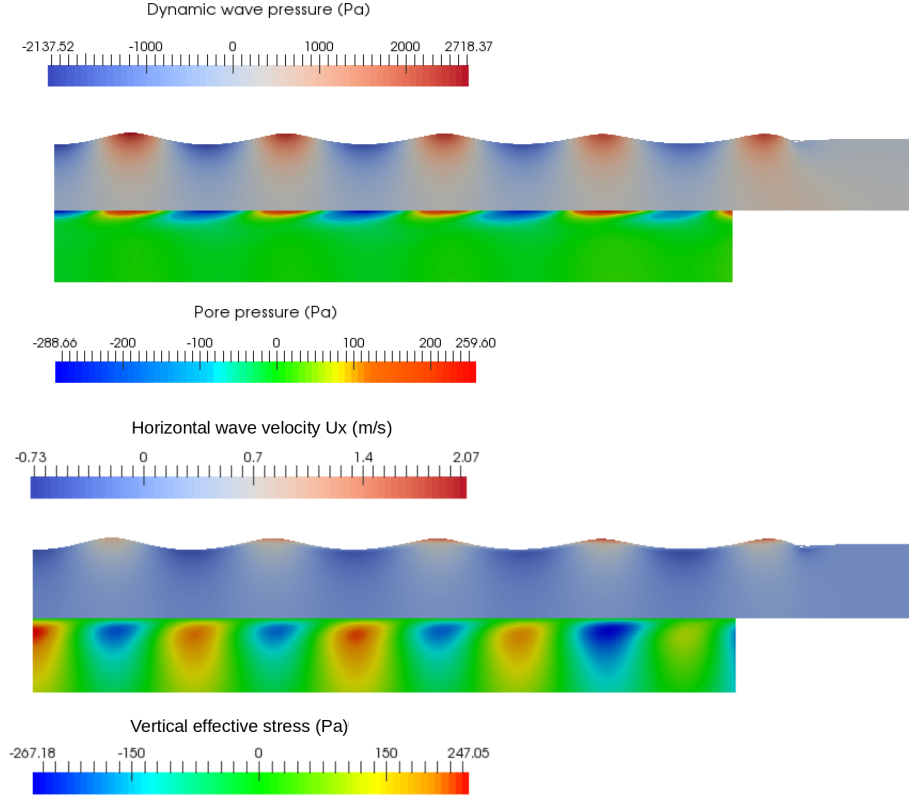
Figure 3.4: Numerical simulation of 2D wave-seabed interaction.

3.3 3D wave-structure-soil interaction

The toolbox including the consolidation solver, WSSI solvers and the liquefaction module ultimately aims to simulate the soil response and momentary liquefaction around marine structures in waves. This tutorial presents the WSSI study for a gravity-based foundations in steep waves. The detailed study and results discussion is presented in Li et al. (2020a). The geometrie of the foundation in the tutorial is shown in Fig. 3.5.
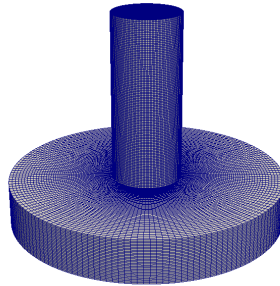

Figure 3.5: Geometry and mesh of the structure.

The entire multiphysics numerical system is established in the 3D Cartesian coordinate system. $z = 0$ is located at the undisturbed free surface. x positive towards the wave propagation direction, y positive towards the side of the tank, and z positive upwards. The layout of the numerical system is shown in Fig. 3.6. The wave inlet relaxation zone is set to be one wave length. The wave outlet relaxation zone is set to 1.25 wave lengths to absorb waves and ensure no reflection from the outlet

boundary. The width of the wave tank (distance between the sides of the tank) is set to be two wave lengths. Table 3.2 gives the parameter settings in the present work.
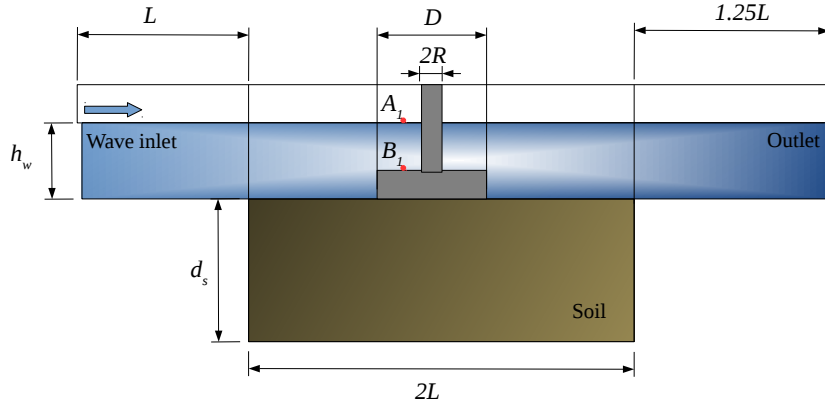

Figure 3.6: A sketch of the numerical layout for the wave-structure-seabed interaction model.

Simulation steps of this tutorial case are as follows:

1. First, the consolidation analysis is performed using `biotConsolidationFoam` to calculate the initial effective stresses distribution in the soil after the completion of soil consolidation process.

2. The wave domain is computed using `waveFoam` to calculate the dynamic wave pressure on the structure and soil.

3. The structure domain is computed using `elasticStructureFoam` to get the structural stress at the structure bottom. Dynamic wave pressure is used as input boundary data.

4. The soil domain is computed to get the soil responses and liquefaction risk. The initial effective stresses from step 1 is used as initial condition in the folder of 0/ (or any time step as start time), i.e. copy the final `initEffSigmaMean` and `initEffSigmazz` from the consolidation case to the initial time folder of the WSSI seabed simulation case. The dynamic wave pressure p and structural stresses σ_S are used as input boundary data in the folder of constant/boundaryData.

Detailed diagram and boundary condition setups are presented in Figs. 2.3 and 2.4. A snapshot of the simulation of WSSI with all three domains (wave, structure, seabed) is generated from paraView and is presented in Fig. 3.7. Results and discussion of this case are presented in Li et al. (2020a,b).

3.4   Momentary liquefaction

Liquefaction criteria as mentioned in Section 2.1.4 are implemented in the soil solvers `anisoUpLiqueFoam` and `anisoBiotLiqueFoam`. The comparison of the liquefaction criteria for analyzing the momentary liquefaction risk around an offshore foundation has performed in Li et al. (2020b).

Table 3.2: Parameter settings for wave-structure-seabed interaction modeling in the present study.

Wave parameters			
Wave height H (m)	4.0		
Wave period T (s)	10.0		
Water depth h_w (m)	10.0		
Wave length L (m)	98.2		
KC number	1.70		
Structure parameters			
Characteristic length D (m)	19.0		
Bottom slab height h_b (m)	3.0		
Shaft radius R (m)	2.25		
Density ρ (kg/m^3)	2400		
Young's modules (N/m^2)	2.2×10^{10}		
Poisson's ratio	0.2		
Seabed parameters		Directional values	
Young's modules (N/m^2)	$E_x = 1.2 \times 10^7$	$E_y = 1.2 \times 10^7$	$E_z = 2 \times 10^7$
Poisson's ratios	$\nu_{xy} = 0.2$	$\nu_{yz} = 0.24$	$\nu_{zx} = 0.4$
Shear modulus (N/m^2)	$G_{xy} = 5 \times 10^6$	$G_{yz} = 1.2 \times 10^7$	$G_{zx} = 1.2 \times 10^7$
Permeabilities(m/s)	$k_x = 0.0005$	$k_y = 0.0005$	$k_z = 0.0001$
Saturation factor S_r	0.98		
Porosity n	0.3		
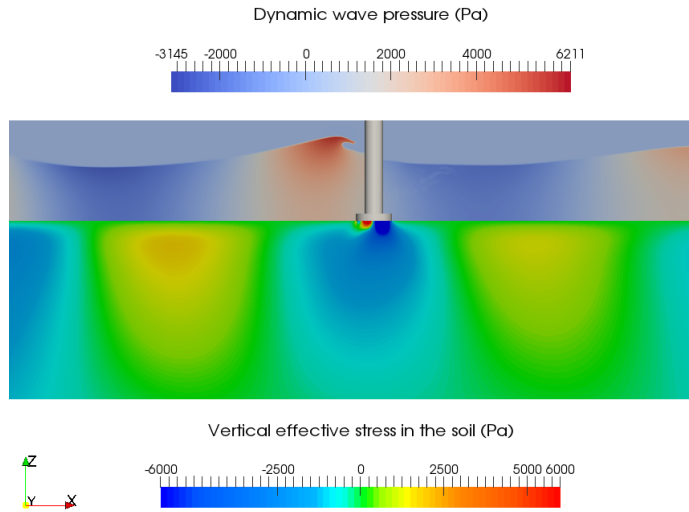
Figure 3.7: Wave crest approaches the structure and generate high opposite vertical stress beneath the structure bottom σ_z (Pa) compared to the nearby field.

Chapter 4

Important remarks

- To use the `anisoUpLiqueFoam` and `anisoBiotLiqueFoam`, the coordination system must set as z-positive towards the vertical upward direction, as $g = (0, 0, -9.82)$ m/s^2.

- The mesh of the consolidation simulation and WSSI-soil simulation shall be the same mesh, in order to copy the `initEffSigmaMean` and `initEffSigmazz` from consolidation case to WSSI-soil case for liquefaction assessment.

- In the 3D-wssi tutorial, the meshes are coarsen in order to make the simulations faster to run as demonstrations. The mesh sizes used in the referred papers are 100 - 1000 times larger than those in the 3D tutorial to achieve accurate results.

- For the liquefaction analysis, only momentary liquefaction can be examined in the present version of the toolbox.

Bibliography

Berberović, E., N. P. van Hinsberg, S. Jakirlić, I. V. Roisman, and C. Tropea
  2009. Drop impact onto a liquid layer of finite thickness: Dynamics of the cavity evolution. *Physical Review E*, 79(3):036306.

Biot, M. A.
  1941. General theory of three-dimensional consolidation. *Journal of applied physics*, 12(2):155–164.

Celli, D., Y. Li, M. C. Ong, and M. Di Risio
  2019. The role of submerged berms on the momentary liquefaction around conventional rubble mound breakwaters. *Applied Ocean Research*, 85:1–11.

Demirdžić, I., I. Horman, and D. Martinović
  2000. Finite volume analysis of stress and deformation in hygro-thermo-elastic orthotropic body. *Computer methods in applied mechanics and engineering*, 190(8):1221–1232.

Demirdžić, I. and D. Martinović
  1993. Finite volume method for thermo-elasto-plastic stress analysis. *Computer Methods in Applied Mechanics and Engineering*, 109(3):331–349.

Demirdžić, I. and S. Muzaferija
  1994. Finite volume method for stress analysis in complex domains. *International Journal for Numerical Methods in Engineering*, 37(21):3751–3766.

Higuera, P., J. L. Lara, and I. J. Losada
  2013. Realistic wave generation and active wave absorption for navier–stokes models: Application to openfoam®. *Coastal Engineering*, 71:102–118.

Jacobsen, N. G., D. R. Fuhrman, and J. Fredsøe
  2012. A wave generation toolbox for the open-source cfd library: Openfoam®. *International Journal for Numerical Methods in Fluids*, 70(9):1073–1088.

Jasak, H. and H. Weller
  2000. Application of the finite volume method and unstructured meshes to linear elasticity. *International journal for numerical methods in engineering*, 48(2):267–287.

Jeng, D.-S.
  1997. Wave-induced seabed instability in front of a breakwater. *Ocean Engineering*, 24(10):887–917.

Li, Y.
  2016. Implementation of multiple time steps for the multi-physics solver based onchtmultiregionfoam. In *CFD with OpenSource Software, 2016, Edited by Nilsson. H.* Chalmers University of Technology.

Li, Y., M. C. Ong, O. T. Gudmestad, and B. H. Hjertager
2020a. The effects of slab geometries and wave directions on the steep wave-induced soil response and liquefaction around gravity-based offshore foundations. *Ships and Offshore Structures*, 15(8):866–877.

Li, Y., M. C. Ong, and T. Tang
2018. Numerical analysis of wave-induced poro-elastic seabed response around a hexagonal gravity-based offshore foundation. *Coastal Engineering*, 136:81–95.

Li, Y., M. C. Ong, and T. Tang
2020b. A numerical toolbox for wave-induced seabed response analysis around marine structures in the openfoam® framework. *Ocean Engineering*, 195:106678.

Okusa, S.
1985. Wave-induced stresses in unsaturated submarine sediments. *Geotechnique*, 35(4):517–532.

Tang, T., B. Johannesson, and J. Roenby
2014. An integrated fvm simulation of wave-seabed-structure interaction using openfoam. In *9th OpenFOAM Workshop, 23-26 June 2014 in Zagreb, Croatia*.

Tsai, C.
1995. Wave-induced liquefaction potential in a porous seabed in front of a breakwater. *Ocean Engineering*, 22(1):1–18.

Vafai, K. and C. Tien
1981. Boundary and inertia effects on flow and heat transfer in porous media. *International Journal of Heat and Mass Transfer*, 24(2):195–203.

Ye, J.
2012. 3D liquefaction criteria for seabed considering the cohesion and friction of soil. *Applied Ocean Research*, 37:111–119.

Ye, J., D.-S. Jeng, R. Wang, and C. Zhu
2013. A 3-D semi-coupled numerical model for fluid–structures–seabed-interaction (FSSI-CAS 3D): Model and verification. *Journal of Fluids and Structures*, 40:148–162.

Zen, K. and H. Yamazaki
1990a. Mechanism of wave-induced liquefaction and densification in seabed. *Soils and Foundations*, 30(4):90–104.

Zen, K. and H. Yamazaki
1990b. Oscillatory pore pressure and liquefaction in seabed induced by ocean waves. *Soils and Foundations*, 30(4):147–161.